

Manipulation of Objects with Tethers and Millirobots

Tiffany Cappellari



Electrical Engineering and Computer Sciences
University of California, Berkeley

Technical Report No. UCB/EECS-2021-53

<http://www2.eecs.berkeley.edu/Pubs/TechRpts/2021/EECS-2021-53.html>

May 12, 2021

Copyright © 2021, by the author(s).
All rights reserved.

Permission to make digital or hard copies of all or part of this work for personal or classroom use is granted without fee provided that copies are not made or distributed for profit or commercial advantage and that copies bear this notice and the full citation on the first page. To copy otherwise, to republish, to post on servers or to redistribute to lists, requires prior specific permission.

Acknowledgement

I would like to thank Professor Ronald Fearing for all his guidance and support in my research for the last few years as well as the members of the Biomimetic Millisystems Lab and Jay Monga for his assistance in running experiments and with control related issues. I would also like to thank Professor Hannah Stuart for agreeing to be the second reader for this thesis and for her input in the editing process.

I am also incredibly grateful to my parents for their unconditional support throughout the entirety of my undergraduate and graduate career thus far and would like to thank them for all the sacrifices they have made so that I could pursue my passions.

Manipulation of Objects with Tethers and Millirobots

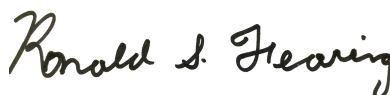
by Tiffany Cappellari

Research Project

Submitted to the Department of Electrical Engineering and Computer Sciences,
University of California at Berkeley, in partial satisfaction of the requirements for the
degree of **Master of Science, Plan II**.

Approval for the Report and Comprehensive Examination:

Committee:



Professor Ronald S. Fearing
Research Advisor

May 11, 2021

(Date)



Professor Hannah Stuart
Second Reader

May 12, 2021

(Date)

Abstract

Manipulation of an Object with Tethers and Millirobots

by

Tiffany Cappellari

Master of Science in Electrical Engineering and Computer Science

University of California, Berkeley

Professor Ronald Fearing, Chair

Robots possess great potential to help people within their homes with a variety of household chores such as organization and picking things up; however, tasks such as these require a high level of dexterity usually found in large, expensive armed robots that would be inconvenient, unaffordable, and intrusive in a typical home. Millirobots, on the other hand, could be a much more viable option as they are more cost effective for the average person and would be smaller, safer, and less obtrusive in the home. Millirobots with the capability to manipulate objects can be used in a number of ways; for example, in the home of a disabled and/or elderly person living alone, these robots can help with everyday tasks that may be difficult for this person to accomplish on their own such as removing tripping hazards, up righting fallen furniture, and fetching hard-to-reach objects. This project explores millirobots' ability to perform grasping and manipulation tasks on larger objects comparable to typical armed robots through the use of tethers and winches. The code can be found at https://github.com/tiffanyec/tether_bots and videos of the experiments can be found at <https://youtu.be/8aOS7uYwEYE>.

Dedicated to the memories of my uncle, who always encouraged me to pursue my passions.

Contents

Contents	ii
List of Figures	iii
List of Tables	v
1 Introduction	1
2 Related Work	3
2.1 Tendon-Driven Hands	3
2.2 Grasping	4
2.3 Robot Cooperation	4
3 Problem Formulation	6
3.1 Geometric Model	6
3.2 Control Model	12
4 Experiments and Setup	15
4.1 Simulation	15
4.2 Experiments	18
5 Results	20
5.1 Velocity vs Torque Controller Comparison	20
6 Discussion and Conclusion	30
Bibliography	32

List of Figures

1.1	A set of millirobots helping a person around their home by removing potential tripping hazards and using tethers to upright a fallen chair. These robots have multi-surface capabilities and can rapidly get out of the person's way. Credit: Hannah Stuart	2
2.1	Examples of tendon driven mechanisms: (a) and (c) are tendon-driven mechanisms, but (b) is not [12].	3
2.2	Quadroters using tethers to lift objects. Left: [13]; Right: CALM [16].	5
2.3	Two robots reorienting a couch [15].	5
3.1	A 2D rectangular object of mass M and length $2r$ suspended in the air by two tethers with tensions t_1 and t_2 .	7
3.2	A 2D rectangular object of mass M and length $2r$ being pulled on the ground by a tether with tension t_1 .	8
3.3	A 2D rectangular object of mass M , length $2r$, and height $2d$ being rotated by two tethers with tensions t_1 and t_2 .	9
3.4	Our simulated robots attached a block object through tether. More detailed figures can be found below at Figure 4.1 and 4.2.	12
3.5	An illustration of the trajectory used to calculate the necessary linear acceleration. A similar method is used to find the angular acceleration.	13
3.6	The overall control block diagram where the input to the system is the desired position and orientation of the block. Only the x position of the block is specified as the goal is to drag it across the ground with the attached tethers acting as the fingers of the grasp and will not lift it, thereby not changing its y -axis position.	14
4.1	A screenshot of the first simulation environment set up. A series of spherical joints and shapes are chained together to create simulated tethers that are attached to a rectangular block object and two wheeled robots. Force sensors measure the tensions of the two tethers.	16
4.2	A screenshot of the second simulation environment set up. The tethers made of spherical joints are now also attached to stiff springs.	16
4.3	Plots comparing the performance of Bullet 2.83 and ODE.	17

5.1	Images of the V-REP simulation before, during, and after rotating the object by -0.5 radians and translating it by 0.3 meters using the velocity controller.	21
5.2	Plots of the results of telling the system to rotate the object by -0.5 radians using the velocity controller. The first two plots show the calculated desired tensions for the two tether t_1 and t_2 needed to generate the necessary forces required to move the block from its current position and orientation to its desired one as well as the system's actual measured tensions at each time step. The bottom two plots show the block's change in position and orientation over time as it converges to approximately the desired values.	22
5.3	Plots of the results of telling the system to move the block object to position 0.2 along the x -axis using the velocity controller. Simply pure translation is not possible with this simulation as the force of friction between the ground and the entire base of the block is too high for the robots to overcome so a small rotation of -0.08 rad is also applied to the object. This very small rotation results in oscillatory behavior once reaching the desired position.	23
5.4	Plots of the results of telling the system to move the block object to position 0.3 along the x -axis and rotate it by -0.5 radians using the velocity controller.	24
5.5	Plots of the results of telling the system to move the block object to position 0.3 along the x -axis and rotate it by -0.6 radians using the velocity controller.	25
5.6	Plots of the results of telling the system to move the block object to position 0.3 along the x -axis and rotate it by -0.4 radians using the velocity controller.	26
5.7	Plots of the results of pure translation of the object by 0.4 m using the torque controller. We can observe that the torque controller exhibits far more oscillatory behavior than the velocity controller. This is most likely due to a combination of a stick-slip friction phenomena, causing the robots to repeatedly need to overcome the force of friction between the block and the ground, as well as the torque controller over-correcting each time it misses its goal. The controller over-correcting could most likely be remedied with further tuning.	27
5.8	A plot of the velocity of the robots and block while translating the block 0.4 m using the torque controller.	28
5.9	Close up snippets of the block angle, the block and robots' positions, and their velocities as the torque controller translates the block 0.4 m. Although only translation is requested, the angle of the block oscillates heavily as the block continuously tips back and forth due to the robots over-correcting in each direction.	29

List of Tables

4.1	Conditions and wrenches needed in order to transform the object by a pure trans-	
	lation, a pure rotation, and by both a rotation and a translation in the set-up	
	depicted in Figure 4.1.	19

Acknowledgments

I would like to thank Professor Ronald Fearing for all his guidance and support in my research for the last few years as well as the members of the Biomimetic Millisystems Lab and Jay Monga for his assistance in running experiments and with control related issues. I would also like to thank Professor Hannah Stuart for agreeing to be the second reader for this thesis and for her input in the editing process.

I am also incredibly grateful to my parents for their unconditional support throughout the entirety of my undergraduate and graduate career thus far and would like to thank them for all the sacrifices they have made so that I could pursue my passions.

Chapter 1

Introduction

Robots have a large amount of potential to help people within their homes with a variety of tasks such as household chores, medical assistance, and education [8], [14]. For example, there are many organization tasks within a home that are high on many people's priority lists such as clearing items around the house as well as picking things up and putting them away [1]. Tasks such as these require a high degree of dexterity that can be easily accomplished with large, industrial robots such as Baxter and Sawyer robots; however, these robots are too large, expensive, and potentially dangerous to become commonplace in a home. Millirobots, however, can possibly be a much more cost effective for the average person and would be smaller, safer, and less intrusive in the home. The main question we want to answer is: Can a team of small, affordable millirobots accomplish the same manipulation tasks as one large, expensive industrial robot?

Millirobots with this capability can be used in a number of ways; for example, in the home of a disabled and/or elderly person living alone, these robots can help with everyday tasks that may be difficult for this person to accomplish on their own such as removing tripping hazards, up righting fallen furniture, and fetching hard-to-reach objects. While being able to use robots to organize furniture in a room is not a new problem [15], millirobots would be much smaller and cheaper than previous robots, making it a much more viable option for the average person to consider as several of these robots could share larger loads in order to generate the necessary forces to move them [2]. These robots could also become scarce when unneeded, unlike larger robots, helping to conserve space and remain unobtrusive. This could be useful with the care and treatment of older adults so that they can still retain independence using these robotic assistants.

This project explores millirobots' capability to perform grasping and manipulation tasks on larger objects through the use of tethers and winches. While the original goal was to validate simulated results through actual robotic experiments, due to the COVID-19 pandemic and the closure of campus and labs, all experiments were performed through simulations instead.

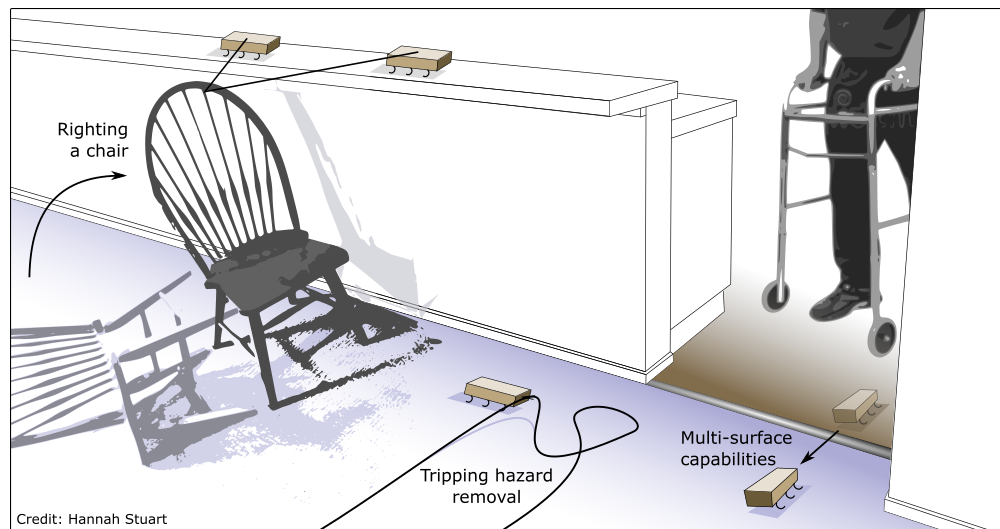


Figure 1.1: A set of millirobots helping a person around their home by removing potential tripping hazards and using tethers to upright a fallen chair. These robots have multi-surface capabilities and can rapidly get out of the person's way. Credit: Hannah Stuart

Chapter 2

Related Work

2.1 Tendon-Driven Hands

Many works explore aspects of the control and manipulation of multifingered robot hands driven by tendons [11], [5], [6], [12], [7]. These hands are designed as underactuated mechanisms using tendons and have a variety of applications such as prostheses and manipulating small objects [12]. A core part of designing and manipulating these robotic hands is controlling the tensions of the tendons in order to apply the necessary forces when using these hands to grasp an object [7]. While these hands also use tension to generate forces for the manipulation of object, these hands are largely used in industrial and otherwise professional environments, not the average person's home, and are more useful for manipulating objects smaller than it rather than larger.

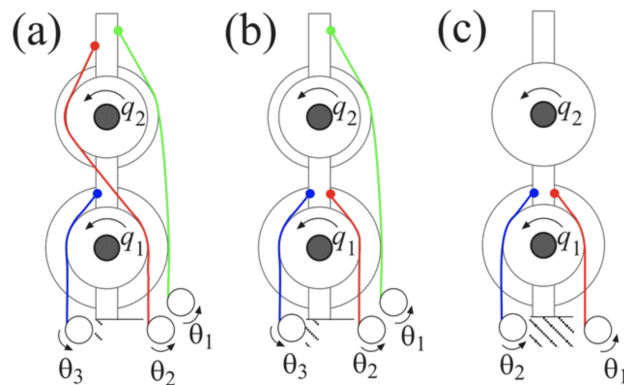


Figure 2.1: Examples of tendon driven mechanisms: (a) and (c) are tendon-driven mechanisms, but (b) is not [12].

2.2 Grasping

Grasping is an important component behavior in how robots can interact with and manipulate objects in order to accomplish desired tasks. The grasp planning problem is to find a set of contact points for the object and the robotic gripper's fingers to both resist external forces and to dextrously manipulate the object [10]. Determining which grasps are better than others is a crucial part of grasp planning as it allows the robot to be able to select the grasp that is most likely to succeed in performing its manipulation task and there are many different grasp quality metrics that can be used to compare different grasps [4]. Studying how human grasping behavior and how humans subconsciously determine grasp forces can also be used to help robots learn how to effectively grasp new objects [9]. Such information can also help us understand and observe how robots can best manipulate objects of any size and shape around them.

2.3 Robot Cooperation

Cooperation among robots can be a great advantage when trying to have smaller robots manipulate larger objects. Several papers explore the concept of using a team of aerial quadrotor robots with tethers to lift and transport objects a single robot would be unable to move [18], [16], [13], [3]. While aerial robotics such as these can have many military and transportation applications [16], they would be inconvenient and unsafe to have indoors and would therefore not be viable for use inside a home. Other papers look to nature for inspiration; for example, ants can work together to transport large amounts of food from one location to another even in environments with unknown and difficult terrain and obstacles [17]. While robots based on ant-like behavior would work together and communicate to accomplish tasks, our project has each robot work independently on its own individual piece of the whole task, making communication between the robots directly unnecessary.

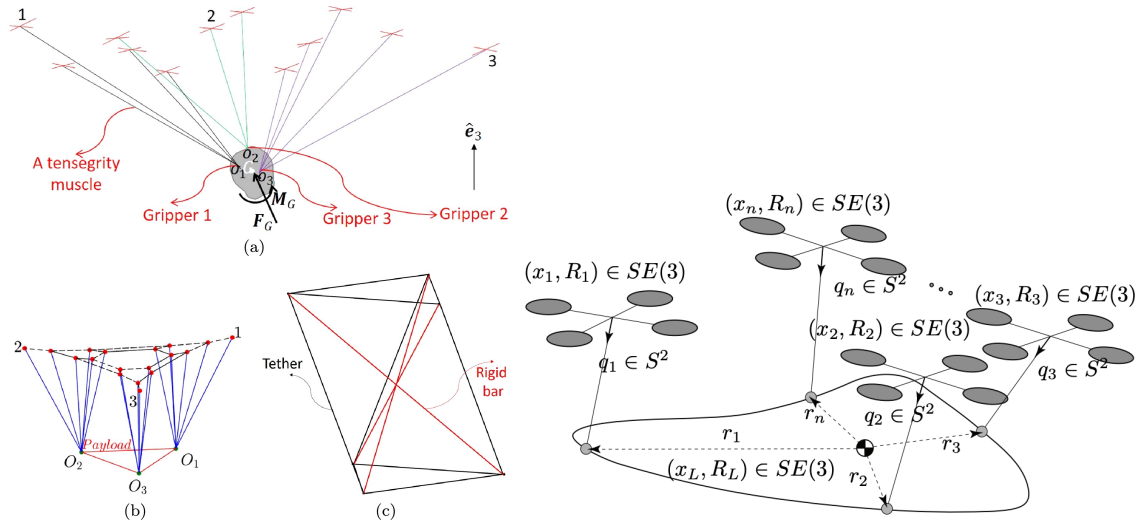


Figure 2.2: Quadroters using tethers to lift objects. Left: [13]; Right: CALM [16].



Figure 2.3: Two robots reorienting a couch [15].

Chapter 3

Problem Formulation

3.1 Geometric Model

2D Case

For a planar, two dimensional grasp, our wrenches are in $SE(2)$. Wrenches in $SE(2)$ are comprised of a linear component, $f \in \mathbb{R}^2$ and an angular component $\tau \in \mathbb{R}$ corresponding to the forces in the plane and to the torque about the normal of the plane, respectively. These wrenches are transformed by

$$\begin{bmatrix} f_O \\ \tau_O \end{bmatrix} = \begin{bmatrix} R_{C_i} & 0 \\ [-p_y & p_x] R_{C_i} & 1 \end{bmatrix} \begin{bmatrix} f_{C_i} \\ \tau_{C_i} \end{bmatrix} \quad (3.1)$$

where R_{C_i} is the rotation of contact point C_i in $SO(2)$ and $p_{C_i} = (p_x, p_y)$ is the location of C_i in \mathbb{R} relative to the object's reference frame.

A grasp is said to be in force closure if it can resist any external applied wrenches [\[10\]](#). In other words, given any external wrench $F \in \mathbb{R}^p$, there exist contact forces $f \in FC$ such that

$$-F = Gf \quad (3.2)$$

Here, f will be a vector of tension forces. The grasp map G is represented by

$$G = [G_{C_1} \quad G_{C_2} \quad \cdots \quad G_{C_n}]$$

where each G_{C_i} is

$$G_{C_i} = Ad_{g_{OC_i}}^T B_{C_i} \quad (3.3)$$

$Ad_{g_{OC_i}}^T$ is the adjoint transpose of the transformation from contact point C_i to the origin of the object O and B_{C_i} is the wrench basis of that contact point. From equation [\[3.1\]](#) we

define

$$Ad_{g_{OC_i}}^T = \begin{bmatrix} R_{C_i} & 0 \\ [-p_y & p_x] R_{C_i} & 1 \end{bmatrix}$$

Example 1: Suspended with Two Tethers

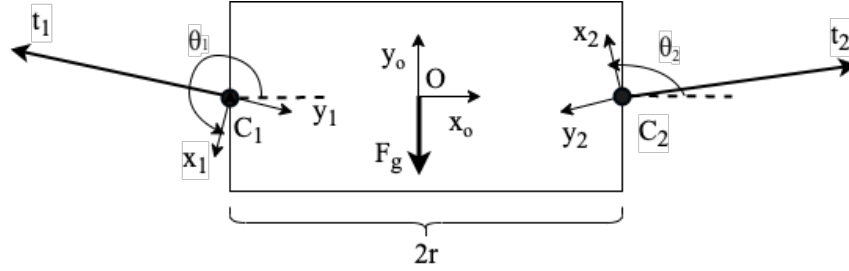


Figure 3.1: A 2D rectangular object of mass M and length $2r$ suspended in the air by two tethers with tensions t_1 and t_2 .

For a frictionless point contact model, the wrench basis $B = \begin{bmatrix} 0 \\ -1 \\ 0 \end{bmatrix}$ has a negative y component because the tension forces are pulling out of the object along the y -axis instead of into the object as with a traditional grasp.

For the grasp depicted in figure [3.1](#) we can model both C_1 and C_2 as frictionless point contacts

$$B_{C_1} = B_{C_2} = \begin{bmatrix} 0 \\ -1 \\ 0 \end{bmatrix}$$

Now we can find the rotation matrices and translation vectors for each tether contact point:

$$\begin{aligned} R_{C_1} &= \begin{bmatrix} \cos \theta_1 & -\sin \theta_1 \\ \sin \theta_1 & \cos \theta_1 \end{bmatrix} & p_{C_1} &= \begin{bmatrix} -r \\ 0 \end{bmatrix} \\ R_{C_2} &= \begin{bmatrix} \cos \theta_2 & -\sin \theta_2 \\ \sin \theta_2 & \cos \theta_2 \end{bmatrix} & p_{C_2} &= \begin{bmatrix} r \\ 0 \end{bmatrix} \end{aligned}$$

Using equation [3.3](#) we find the grasp matrix for each C_i and combine them to get the

overall grasp matrix for the system:

$$G_1 = \begin{bmatrix} \cos \theta_1 & -\sin \theta_1 & 0 \\ \sin \theta_1 & \cos \theta_1 & 0 \\ -r \sin \theta_1 & -r \cos \theta_1 & 1 \end{bmatrix} \begin{bmatrix} 0 \\ -1 \\ 0 \end{bmatrix} = \begin{bmatrix} \sin \theta_1 \\ -\cos \theta_1 \\ r \cos \theta_1 \end{bmatrix}$$

$$G_2 = \begin{bmatrix} \cos \theta_2 & -\sin \theta_2 & 0 \\ \sin \theta_2 & \cos \theta_2 & 0 \\ r \sin \theta_2 & r \cos \theta_2 & 1 \end{bmatrix} \begin{bmatrix} 0 \\ -1 \\ 0 \end{bmatrix} = \begin{bmatrix} \sin \theta_2 \\ -\cos \theta_2 \\ -r \cos \theta_2 \end{bmatrix}$$

$$G = [G_1 \ G_2] = \begin{bmatrix} \sin \theta_1 & \sin \theta_2 \\ -\cos \theta_1 & -\cos \theta_2 \\ r \cos \theta_1 & -r \cos \theta_2 \end{bmatrix}$$

Plugging into equation [3.2](#) we get

$$\begin{bmatrix} 0 \\ Mg \\ 0 \end{bmatrix} = \begin{bmatrix} \sin \theta_1 & \sin \theta_2 \\ -\cos \theta_1 & -\cos \theta_2 \\ r \cos \theta_1 & -r \cos \theta_2 \end{bmatrix} \begin{bmatrix} t_1 \\ t_2 \end{bmatrix}$$

where t_1 and t_2 are the tensions of each tether. We want $-F = \begin{bmatrix} 0 \\ Mg \\ 0 \end{bmatrix}$ since our goal with this grasp is to suspend the object and so the only outside force we want to resist is gravity in along the y -axis.

Example 2: Pulled by One Tether on Ground

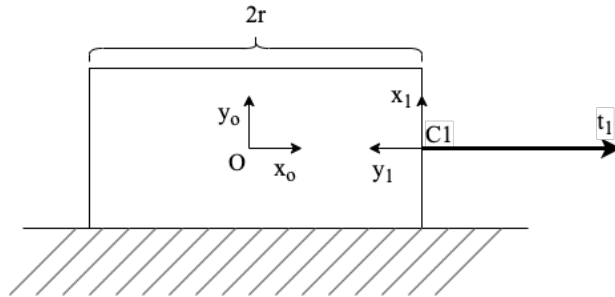


Figure 3.2: A 2D rectangular object of mass M and length $2r$ being pulled on the ground by a tether with tension t_1 .

Letting the friction constant of the object on the ground be μ , for the tether to be able to move the object, it only needs to overcome the resistive frictional force $Mg\mu$ where g is

the acceleration of gravity. Therefore, for the block to move we need $t_1 > Mg\mu$. Using the previous section, we get our grasp map here to simply be

$$G = \begin{bmatrix} 0 & -1 & 0 \\ 1 & 0 & 0 \\ r & 0 & 1 \end{bmatrix} \begin{bmatrix} 0 \\ -1 \\ 0 \end{bmatrix} = \begin{bmatrix} 1 \\ 0 \\ 0 \end{bmatrix}$$

The only force we want it to be able to resist is the force of friction therefore our system of equations becomes

$$\begin{bmatrix} Mg\mu \\ 0 \\ 0 \end{bmatrix} = \begin{bmatrix} 1 \\ 0 \\ 0 \end{bmatrix} t_1$$

This again gives us the conclusion that we need $t_1 > Mg\mu$ in order for the block to overcome friction and move.

Example 3: Held by Two Tethers with Fixed Point on Ground with Friction

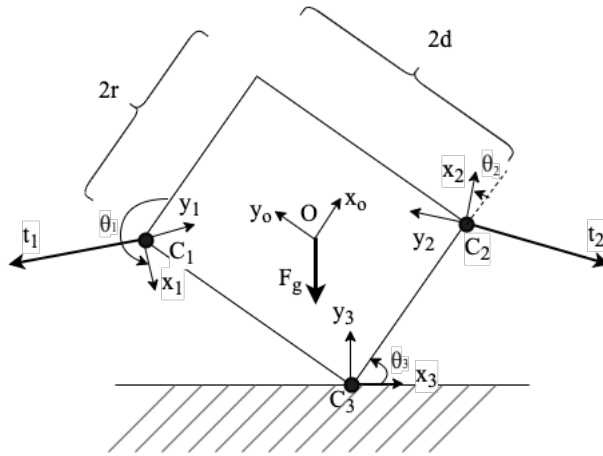


Figure 3.3: A 2D rectangular object of mass M , length $2r$, and height $2d$ being rotated by two tethers with tensions t_1 and t_2 .

Here, the wrench bases for C_1 and C_2 are the same as in the previous section, however, we are now modelling the object's contact point on the ground as a point contact with friction

so the wrench basis will be $B_3 = \begin{bmatrix} 1 & 0 \\ 0 & 1 \\ 0 & 0 \end{bmatrix}$.

The rotation matrices and translation vectors for each contact point of the grasp are:

$$\begin{aligned} R_{C_1} &= \begin{bmatrix} \cos \theta_1 & -\sin \theta_1 \\ \sin \theta_1 & \cos \theta_1 \end{bmatrix} & p_{C_1} &= \begin{bmatrix} -r \\ d \end{bmatrix} \\ R_{C_2} &= \begin{bmatrix} \cos \theta_2 & -\sin \theta_2 \\ \sin \theta_2 & \cos \theta_2 \end{bmatrix} & p_{C_2} &= \begin{bmatrix} r \\ -d \end{bmatrix} \\ R_{C_3} &= \begin{bmatrix} \cos \theta_3 & -\sin \theta_3 \\ \sin \theta_3 & \cos \theta_3 \end{bmatrix} & p_{C_3} &= \begin{bmatrix} -r \\ -d \end{bmatrix} \end{aligned}$$

Using equation 3.3 we find the grasp matrix for each tether and combine them to get the overall grasp matrix for this system:

$$\begin{aligned} G_1 &= \begin{bmatrix} \cos \theta_1 & -\sin \theta_1 & 0 \\ \sin \theta_1 & \cos \theta_1 & 0 \\ -d \cos \theta_1 - r \sin \theta_1 & d \sin \theta_1 - r \cos \theta_1 & 1 \end{bmatrix} \begin{bmatrix} 0 \\ -1 \\ 0 \end{bmatrix} = \begin{bmatrix} \sin \theta_1 \\ -\cos \theta_1 \\ -d \sin \theta_1 + r \cos \theta_1 \end{bmatrix} \\ G_2 &= \begin{bmatrix} \cos \theta_2 & -\sin \theta_2 & 0 \\ \sin \theta_2 & \cos \theta_2 & 0 \\ d \cos \theta_2 + r \sin \theta_2 & -d \sin \theta_2 + r \cos \theta_2 & 1 \end{bmatrix} \begin{bmatrix} 0 \\ -1 \\ 0 \end{bmatrix} = \begin{bmatrix} \sin \theta_2 \\ -\cos \theta_2 \\ d \sin \theta_2 - r \cos \theta_2 \end{bmatrix} \\ G_3 &= \begin{bmatrix} \cos \theta_3 & -\sin \theta_3 & 0 \\ \sin \theta_3 & \cos \theta_3 & 0 \\ d \cos \theta_3 - r \sin \theta_3 & -d \sin \theta_3 - r \cos \theta_3 & 1 \end{bmatrix} \begin{bmatrix} 1 & 0 \\ 0 & 1 \\ 0 & 0 \end{bmatrix} = \begin{bmatrix} \cos \theta_3 & -\sin \theta_3 \\ \sin \theta_3 & \cos \theta_3 \\ -r \sin \theta_3 + d \cos \theta_3 & -r \cos \theta_3 - d \sin \theta_3 \end{bmatrix} \\ G &= \begin{bmatrix} \sin \theta_1 & \sin \theta_2 & \cos \theta_3 & -\sin \theta_3 \\ -\cos \theta_1 & -\cos \theta_2 & \sin \theta_3 & \cos \theta_3 \\ -d \sin \theta_1 + r \cos \theta_1 & d \sin \theta_2 - r \cos \theta_2 & -r \sin \theta_3 + d \cos \theta_3 & -r \cos \theta_3 - d \sin \theta_3 \end{bmatrix} \end{aligned}$$

Since C_3 is modelled with friction, we can write the friction cone constraint as

$$\begin{aligned} f_{C_3} &\in FC_{C_3} \\ FC_{C_3} &= \{f \in \mathbb{R} : |f_1| \leq \mu f_2, f_2 \geq 0\} \end{aligned} \quad (3.4)$$

Since the third contact point is the ground pushing into the object, we can set f_2 of C_3 to be $Mg \sin \theta_3$. In order to suspend the block in its current position, the only force we want our grasp to resist is the torque caused by gravity: $\tau_g = Mgd \cos \theta_3$. Plugging into equation 3.2 we get

$$\begin{bmatrix} 0 \\ 0 \\ \tau_g \end{bmatrix} = \begin{bmatrix} \sin \theta_1 & \sin \theta_2 & \cos \theta_3 & -\sin \theta_3 \\ -\cos \theta_1 & -\cos \theta_2 & \sin \theta_3 & \cos \theta_3 \\ -d \sin \theta_1 + r \cos \theta_1 & d \sin \theta_2 - r \cos \theta_2 & -r \sin \theta_3 + d \cos \theta_3 & -r \cos \theta_3 - d \sin \theta_3 \end{bmatrix} \begin{bmatrix} t_1 \\ t_2 \\ f_1 \\ f_2 \end{bmatrix}$$

This grasp is in force closure since $G(FC) = \mathbb{R}^3$, however, since we are using quasi-static analysis for this project, this system of equations is statically indeterminate as it is under constrained.

Example 4: Held by Two Tethers with Fixed Point on Ground without Friction

In order to further simplify the previous case so in order to get a solvable system of equations, we can model C_3 as a frictionless point contact. As the system is quasi-static, we can ignore friction at the point contact between the object and the ground. In this case, G_1 and G_2 will remain the same as before but G_3 will now be

$$G_3 = \begin{bmatrix} \cos \theta_3 & -\sin \theta_3 & 0 \\ \sin \theta_3 & \cos \theta_3 & 0 \\ d \cos \theta_3 - r \sin \theta_3 & -d \sin \theta_3 - r \cos \theta_3 & 1 \end{bmatrix} \begin{bmatrix} 0 \\ 1 \\ 0 \end{bmatrix} = \begin{bmatrix} -\sin \theta_3 \\ \cos \theta_3 \\ -d \sin \theta_3 - r \cos \theta_3 \end{bmatrix}$$

making our new grasp map and equation

$$\begin{bmatrix} 0 \\ 0 \\ \tau_g \end{bmatrix} = \begin{bmatrix} \sin \theta_1 & \sin \theta_2 & -\sin \theta_3 \\ -\cos \theta_1 & -\cos \theta_2 & \cos \theta_3 \\ -d \sin \theta_1 + r \cos \theta_1 & d \sin \theta_2 - r \cos \theta_2 & -d \sin \theta_3 - r \cos \theta_3 \end{bmatrix} \begin{bmatrix} t_1 \\ t_2 \\ f_1 \end{bmatrix}$$

where f_1 is now the force the ground is applying into the object at point C_3 . We can observe that this simplified grasp is still in force closure. For the following controls and experiments in this paper, we will use this grasp map and model to do all calculations.

Moving the Block

In order to move the block to a desired position and orientation, we now need our grasp to also apply a translational force and a torque that will overcome the force of gravity instead of just resisting it. These necessary forces will become our new desired wrench:

$$-F = \begin{bmatrix} F_x \\ F_y \\ \tau \end{bmatrix}$$

where F_x is the force along the x -axis, F_y is the force along the y -axis, and τ is the torque applied to the object. Using Example 4's model, we get our new system of equations to be

$$\begin{bmatrix} F_x \\ F_y \\ \tau \end{bmatrix} = \begin{bmatrix} \sin \theta_1 & \sin \theta_2 & -\sin \theta_3 \\ -\cos \theta_1 & -\cos \theta_2 & \cos \theta_3 \\ -d \sin \theta_1 + r \cos \theta_1 & d \sin \theta_2 - r \cos \theta_2 & -d \sin \theta_3 - r \cos \theta_3 \end{bmatrix} \begin{bmatrix} t_1 \\ t_2 \\ f_1 \end{bmatrix} \quad (3.5)$$

Since we are only interested in dragging the object across the ground with the tethers, we can set $F_y = 0$. Solving for t_1 and t_2 we can find the necessary tether tensions needed to apply the desired wrench to the object.

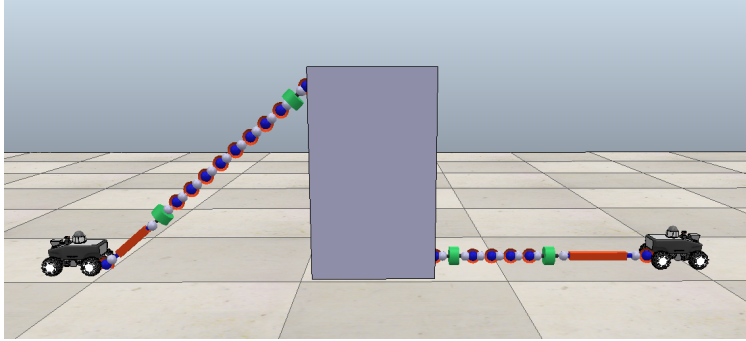


Figure 3.4: Our simulated robots attached a block object through tether. More detailed figures can be found below at Figure [4.1](#) and [4.2](#).

We now need a way to actually apply the calculated necessary tensions to the tethers in order to manipulate the object. Ideally in the future we would want to use winches to apply the tensions and robots to connect the object to the winches with tethers. For this project, however, we will be using wheeled robots in order to create the necessary forces to grasp the object; the following section will go into more detail on how to control these robots. An image of our set-up can be viewed in Figure [3.4](#).

3.2 Control Model

The previous section showed that tensions can be used to grasp and manipulate objects. This section will describe our controller design to use robots to apply the necessary tensions to transform the object in a planar space. Like before, we define the desired wrench of the forces and torque we want to apply to the object as

$$-F = \begin{bmatrix} F_x \\ F_y \\ \tau \end{bmatrix} \quad (3.6)$$

and we can find our desired fingertip forces using

$$-F = Gf$$

again where G is the grasp map and $f \in \mathbb{R}^3$ are the forces of the fingertips. As previously mentioned, because we are only interested in using the tethers to drag the object across the ground rather than lift it, we can disregard F_y by setting it to 0.

In order to find the desired wrench F given a desired x position and orientation of the object, we need to calculate the necessary linear (F) and angular (τ) forces to move the

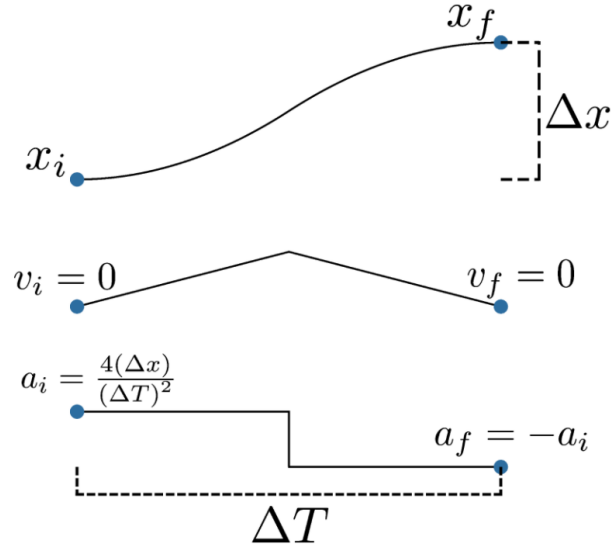


Figure 3.5: An illustration of the trajectory used to calculate the necessary linear acceleration. A similar method is used to find the angular acceleration.

object towards the desired transformation. Since the system is quasi-static, we can use a piecewise-polynomial trajectory to calculate the necessary linear and angular accelerations using instantaneous acceleration. A depiction of this can be seen in Figure 3.5. The following equations were used to find the accelerations, force, and torque needed from the robots

$$\begin{aligned} \tau &= I\alpha & F &= Ma \\ \alpha &= \frac{4(\Delta\theta)}{T^2} & a &= \frac{4(\Delta x)}{T^2} \end{aligned}$$

where I is the moment of inertia of the object, α is its angular acceleration, a is its linear acceleration, M is the object's mass, ΔT is the amount of time over which we want to complete the action, and $\Delta\theta$ and Δx are the differences in the current and desired angle and position, respectively.

Now with a desired wrench F and our known grasp map, we can use the inverse of G to find our desired tensions in f as $G \in \mathbb{R}^{3 \times 3}$ and is invertible

$$f = -G^{-1}F \quad (3.7)$$

Using the desired tensions $t_{1,d}$ and $t_{2,d}$ for the two tethers, we can then control the robots to move until they achieve the desired tensions for their respective tethers. Once the tensions are achieved, the position and orientation of the object is checked for accuracy and the next

wrench is computed to further move the object if necessary.

After the object has achieved the user's inputted position and orientation, the robots then act to keep the object in place and only need to resist the torque caused by gravity, much like in Example 4 in section 3.1. A block diagram of the overall control model can be seen in Figure 3.6.

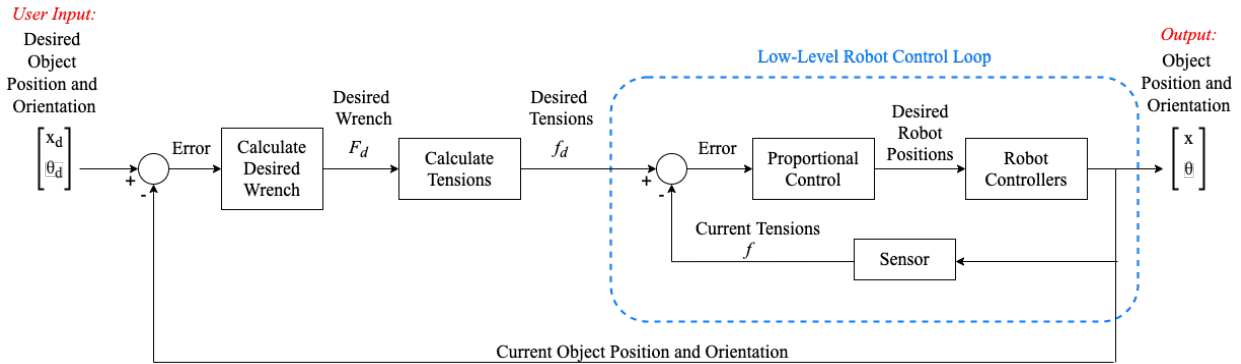


Figure 3.6: The overall control block diagram where the input to the system is the desired position and orientation of the block. Only the x position of the block is specified as the goal is to drag it across the ground with the attached tethers acting as the fingers of the grasp and will not lift it, thereby not changing its y -axis position.

Robot Controllers: Velocity vs Torque Control

To control each individual robot in order to achieve the desired tensions of each tether, we have two options of controllers: velocity and torque control. This additional controller can be seen in Figure 3.6 inside the low-level robot control loop as Robot Controllers. Each robot has its own instance of this controller and controls itself independently of the other robot.

We first created a velocity controller that first used proportional control on the tensions error to determine the distance to move the robot before calculating the desired velocity of each wheel and sending them to the built in sub-controllers included in the V-REP simulation. We then created a torque controller for the wheels of the robots that sent torque commands directly to V-REP's controllers.

Chapter 4

Experiments and Setup

4.1 Simulation

All of the experiments performed and described in this paper were done in the simulation engine V-REP. As there are no simulated tethers or ropes included in V-REP, we created our own by chaining together spherical joints together with force sensors attached at each end to measure the tension of the tether. This allowed us to model the flexibility of a tether and in a later set-up we also added stiff springs to model the small amount of spring force a real tether would exhibit. For the robots, we used V-REP's included Robotnik Summit XL car model to act in place of winches that would apply the necessary forces to transform the object. An image of this simulation can be seen in Figure [4.1](#).

Bullet vs ODE Physics Engine

To simulate the physics of our system, we had two options: Bullet 2.83 and Open Dynamics Engine (ODE). Both Bullet and ODE are open-source physics engines that can be used to simulate the physics and dynamics of our V-REP experiments.

Using the setup depicted in Figure [4.1](#), we tested both physics engines and measured the tensions of the tethers over time. We let the robots drive forward using a default controller provided by V-REP until the object was rotated 180 deg and lay on the ground on its side. The results of these measurements can be observed in Figure [4.3](#).

We observed that Bullet's results were overall smoother and more consistent than ODE's results. Based on these tests, we made the decision to use Bullet 2.83 for our following experiments.

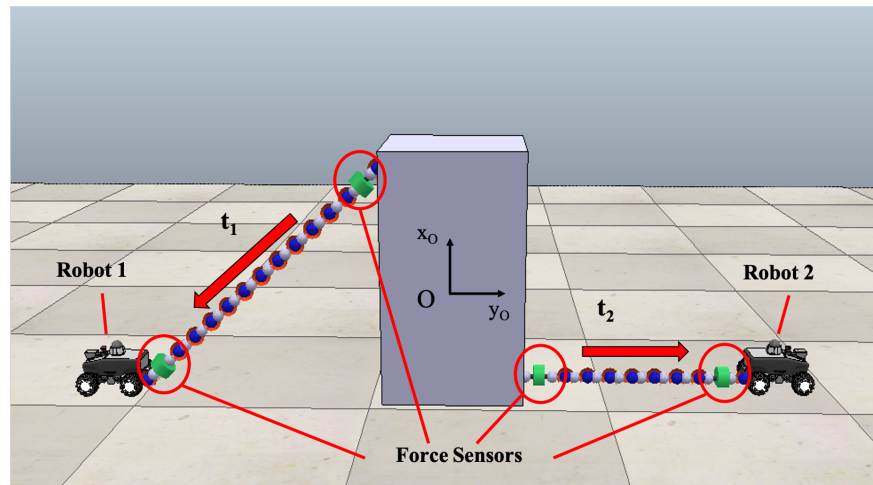


Figure 4.1: A screenshot of the first simulation environment set up. A series of spherical joints and shapes are chained together to create simulated tethers that are attached to a rectangular block object and two wheeled robots. Force sensors measure the tensions of the two tethers.

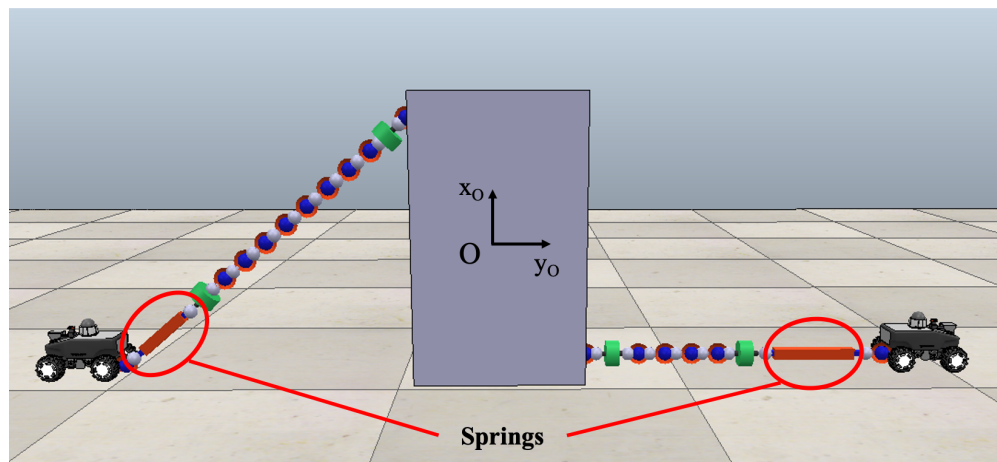
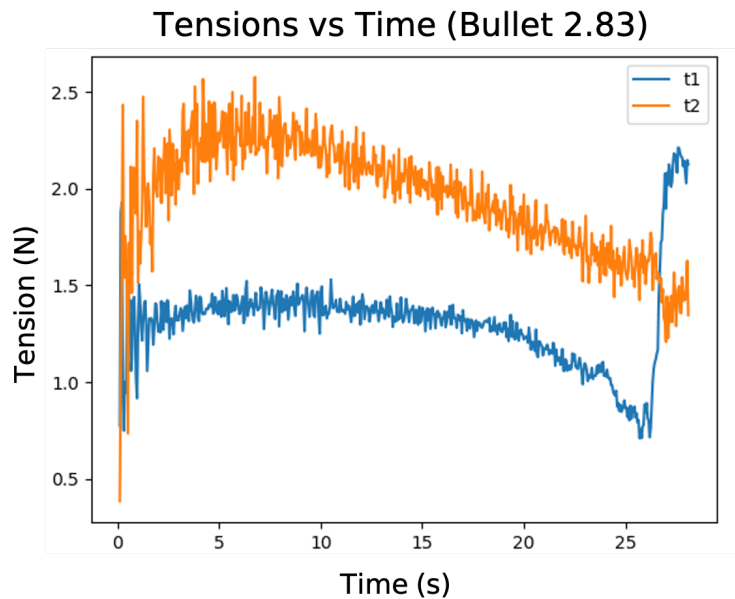


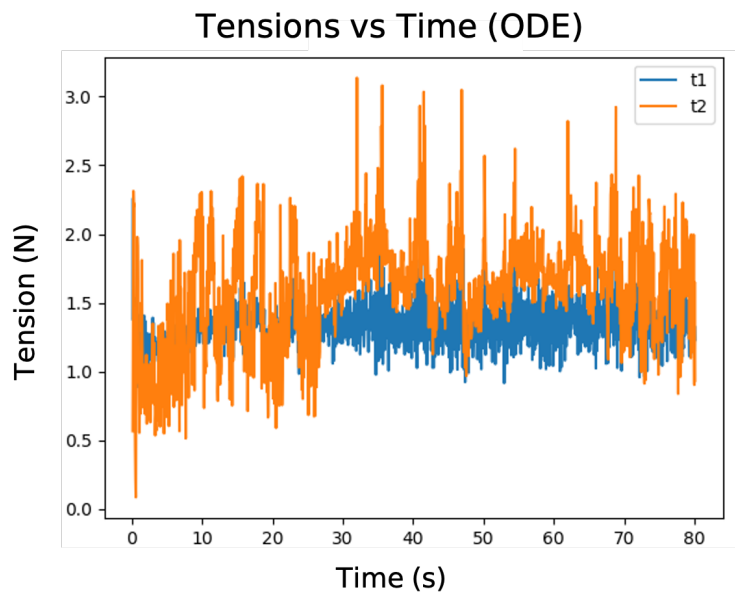
Figure 4.2: A screenshot of the second simulation environment set up. The tethers made of spherical joints are now also attached to stiff springs.

Robotic Operating System (ROS)

Robotic Operating System (ROS) is an open-source set of software libraries used to build robot applications. ROS creates a subscriber-publisher relationship between nodes through topics. The publisher will send information to a topic and the subscriber will continuously read the topic and run a callback function whenever information is received.



(a) A plot of the tensions vs time using Bullet 2.83.



(b) A plot of the tensions vs time using ODE.

Figure 4.3: Plots comparing the performance of Bullet 2.83 and ODE.

For this project, we used ROS mainly because of its asynchronicity and organization. While V-REP sent all position, tension, and orientation information to the Python backend,

the Python script performed all necessary calculations and sent back the necessary robot velocities and torques. As we have more than one robot needing to work in parallel, ROS's asynchronous aspect was useful in controlling all of the robots at once.

4.2 Experiments

To test our control scheme, we tested how well the robots could translate and rotate the object to a desired position and orientation within a specified tolerance. For the trivial cases, we had the robots move the block by 0.3 meters with no rotation and rotate the object by -0.5 radians with no translation. For the nontrivial cases, the robots attempted to transform the object to three user-specified positions and orientations. In total, the following transformations were applied to the object with both the velocity and torque controllers for the robots:

- -0.5 radians
- 0.3 meters
- -0.5 radians and 0.3 meters
- -0.6 radians and 0.3 meters
- -0.4 radians and 0.3 meters

A table of necessary conditions and wrenches needed to achieve these different types of transformations can be found in Table [4.1](#).

Desired Object Movement	Desired Wrench	Necessary Conditions
Pure Translation	$F = \begin{bmatrix} F_x \\ 0 \\ 0 \end{bmatrix}$	The tension of robot2 must overcome the force of friction between the object and the ground in order to slide the object to the target position.
Pure Rotation	$F = \begin{bmatrix} 0 \\ 0 \\ \tau \end{bmatrix}$	The net force applied to the block from the two robots along the x-axis must be less than the force of friction between the object and the ground in order to avoid slipping. The torque caused by the the robots pulling on the tethers also need to be larger than the opposing torque caused by gravity in order to overcome the force of gravity and rotate the object.
Rotation and Translation	$F = \begin{bmatrix} F_x \\ 0 \\ \tau \end{bmatrix}$	The net force on the block along the x-axis must be greater than the resisting force of friction and the torque applied to object must also be greater than the torque caused by the force of gravity in order for the block to both translate and rotate.

Table 4.1: Conditions and wrenches needed in order to transform the object by a pure translation, a pure rotation, and by both a rotation and a translation in the set-up depicted in Figure [4.1](#).

Chapter 5

Results

5.1 Velocity vs Torque Controller Comparison

As discussed in the previous section, we tested our control scheme on three different cases: pure rotation, pure translation, and both rotation and translation with three different sets of target values for the final case. Plots of the object's position and orientation, the robots' positions, and the desired and actual tensions can be observed below. For the robot controller, we tested both a velocity controller and a torque controller. Results for the velocity controller experiments can be found in Figures [5.2](#), [5.3](#), [5.4](#), [5.5](#), and [5.6](#). Results for the torque controller experiments can be found in Figures [5.7](#), [5.8](#) and [5.9](#). Videos of some of the experiments can be found at <https://youtu.be/8aOS7uYwEYE>.

While the velocity controller was able to move the object to the desired positions and orientations specified, it struggled with suddenly changing directions when the tension of the robot's tether was too high or too low and the robot had to reverse directions to remedy the difference. This problem often presented itself when the robots needed to balance the object at the goal transformation. The torque controller, on the other hand, exhibited far more oscillations as it tried to move the object but was able to converge to the goal state much faster. In order to help mediate the oscillation problem, we added a derivative component to the torque controller making it a PD controller compared to the velocity controller's purely proportional control. We also observed that the addition of the springs in the tethers were increasing the oscillation of the system, making it more difficult for the robots to balance the object at the goal and so we used the original simulation set-up depicted in Figure [4.1](#) rather than the one in [4.2](#). We suspect this is most likely due to some unstable dynamics within the simulation environment.

Overall, the torque controller can converge to the given goal faster but is less stable, has more oscillations, and is more sensitive to errors compared to the velocity controller. The greater instability is most likely largely due to torque control being at a lower level than

velocity control causing a slower response to disturbances. This increased sensitivity to error caused the torque controller to continually over-correct when missing its target, causing it to oscillate about its goal.

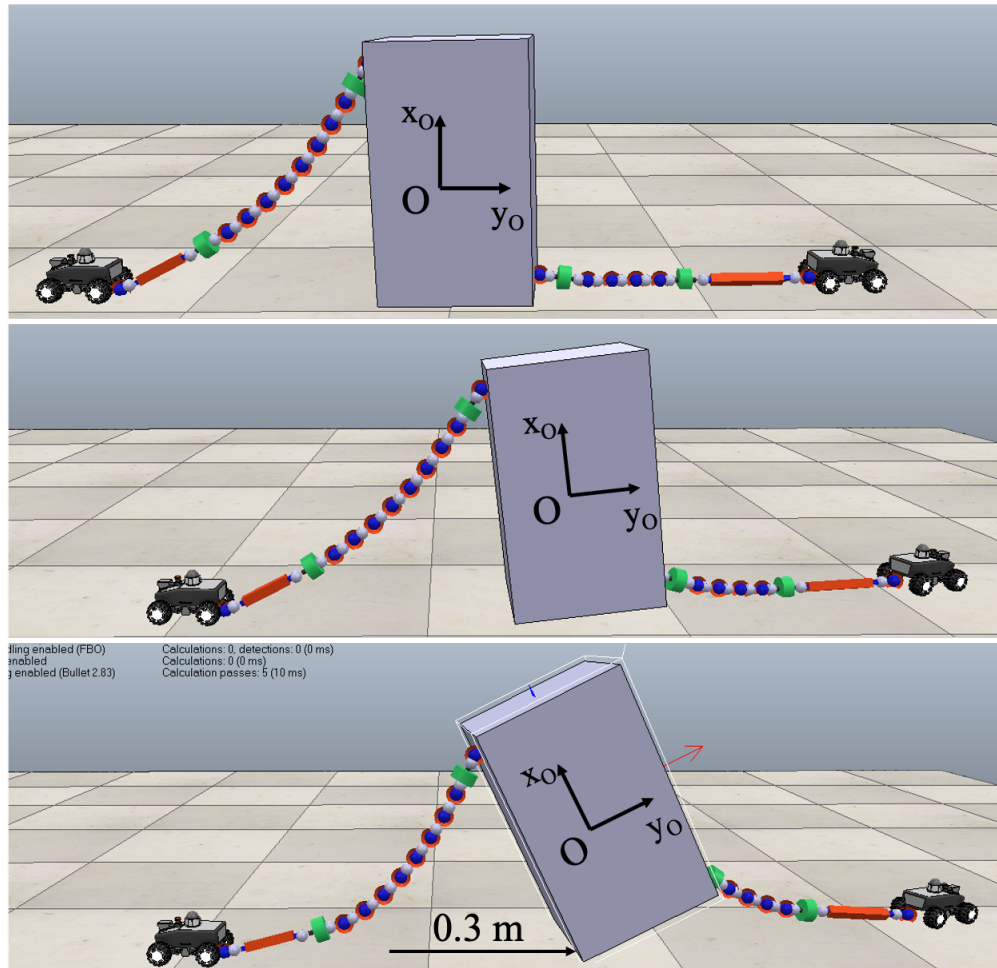


Figure 5.1: Images of the V-REP simulation before, during, and after rotating the object by -0.5 radians and translating it by 0.3 meters using the velocity controller.

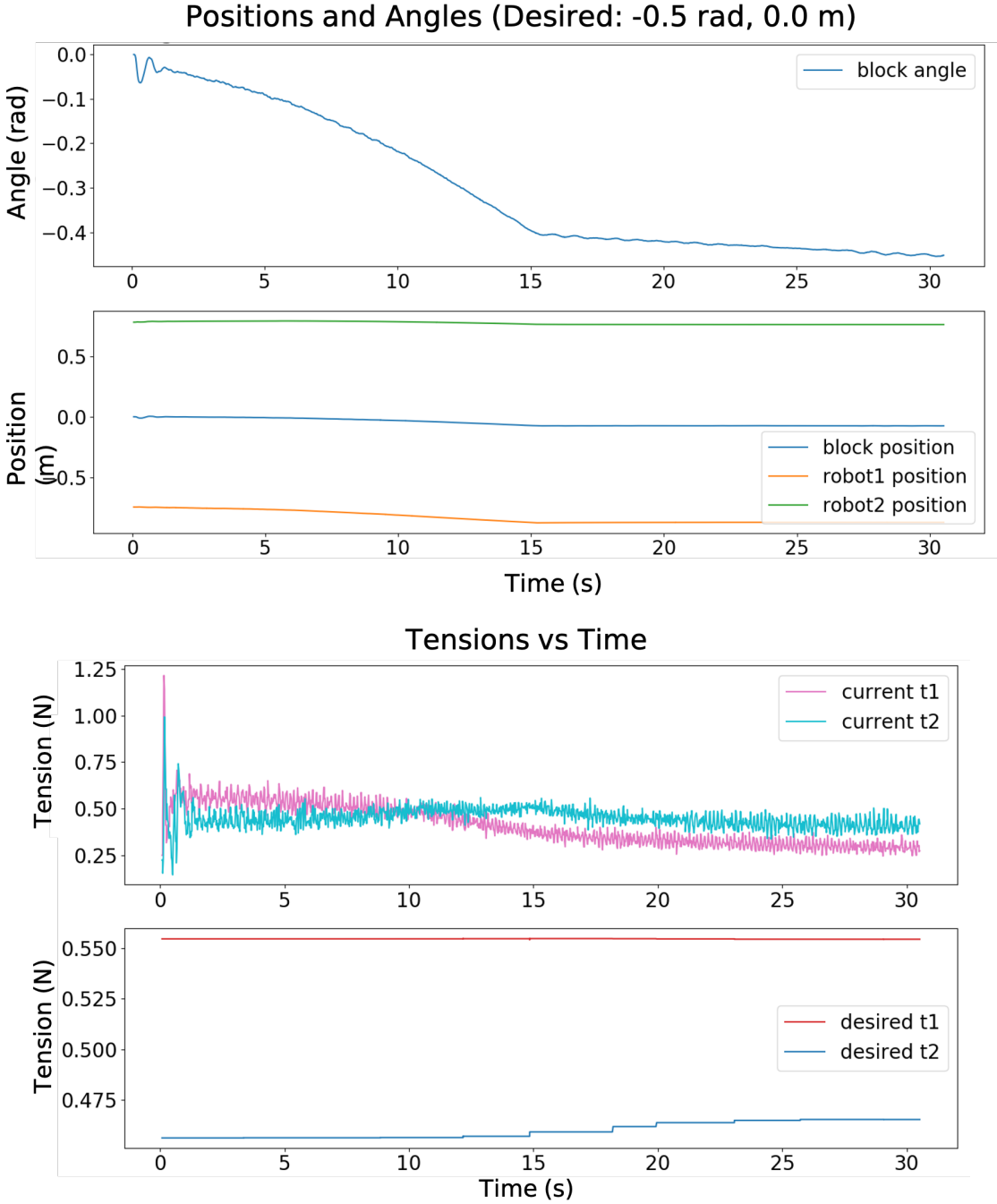


Figure 5.2: Plots of the results of telling the system to rotate the object by -0.5 radians using the velocity controller. The first two plots show the calculated desired tensions for the two tether t_1 and t_2 needed to generate the necessary forces required to move the block from its current position and orientation to its desired one as well as the system's actual measured tensions at each time step. The bottom two plots show the block's change in position and orientation over time as it converges to approximately the desired values.

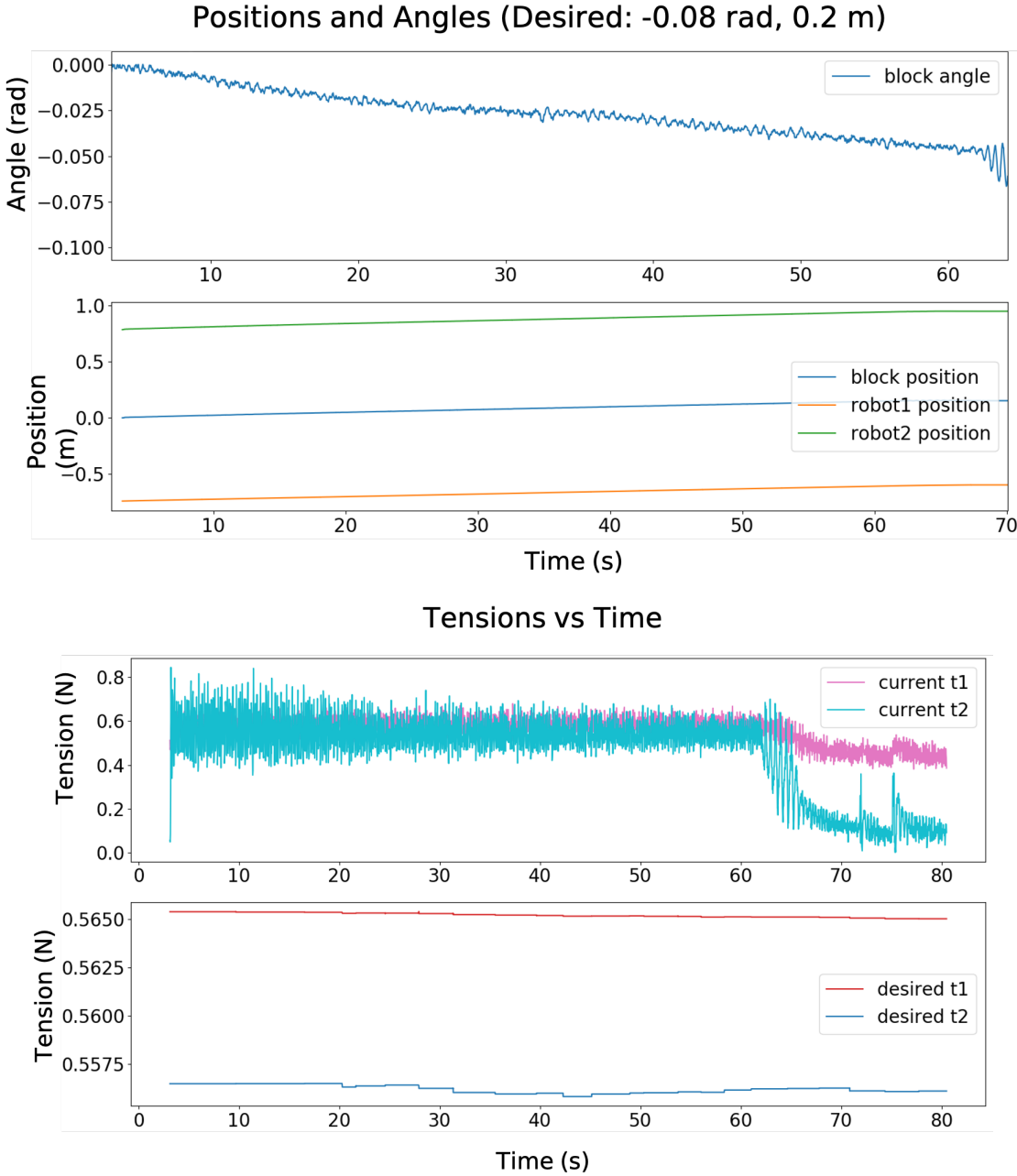


Figure 5.3: Plots of the results of telling the system to move the block object to position 0.2 along the x -axis using the velocity controller. Simply pure translation is not possible with this simulation as the force of friction between the ground and the entire base of the block is too high for the robots to overcome so a small rotation of -0.08 rad is also applied to the object. This very small rotation results in oscillatory behavior once reaching the desired position.

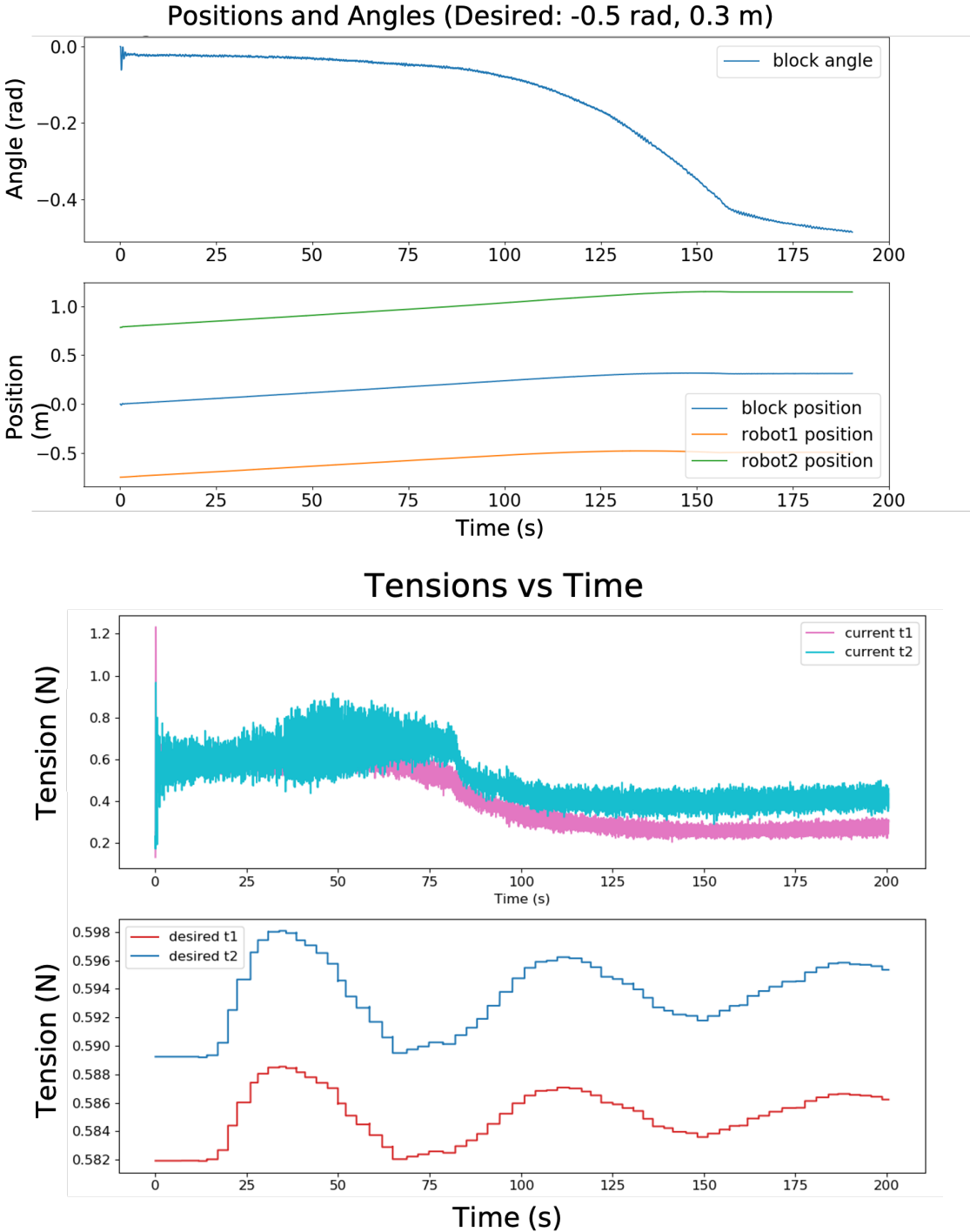


Figure 5.4: Plots of the results of telling the system to move the block object to position 0.3 along the x -axis and rotate it by -0.5 radians using the velocity controller.

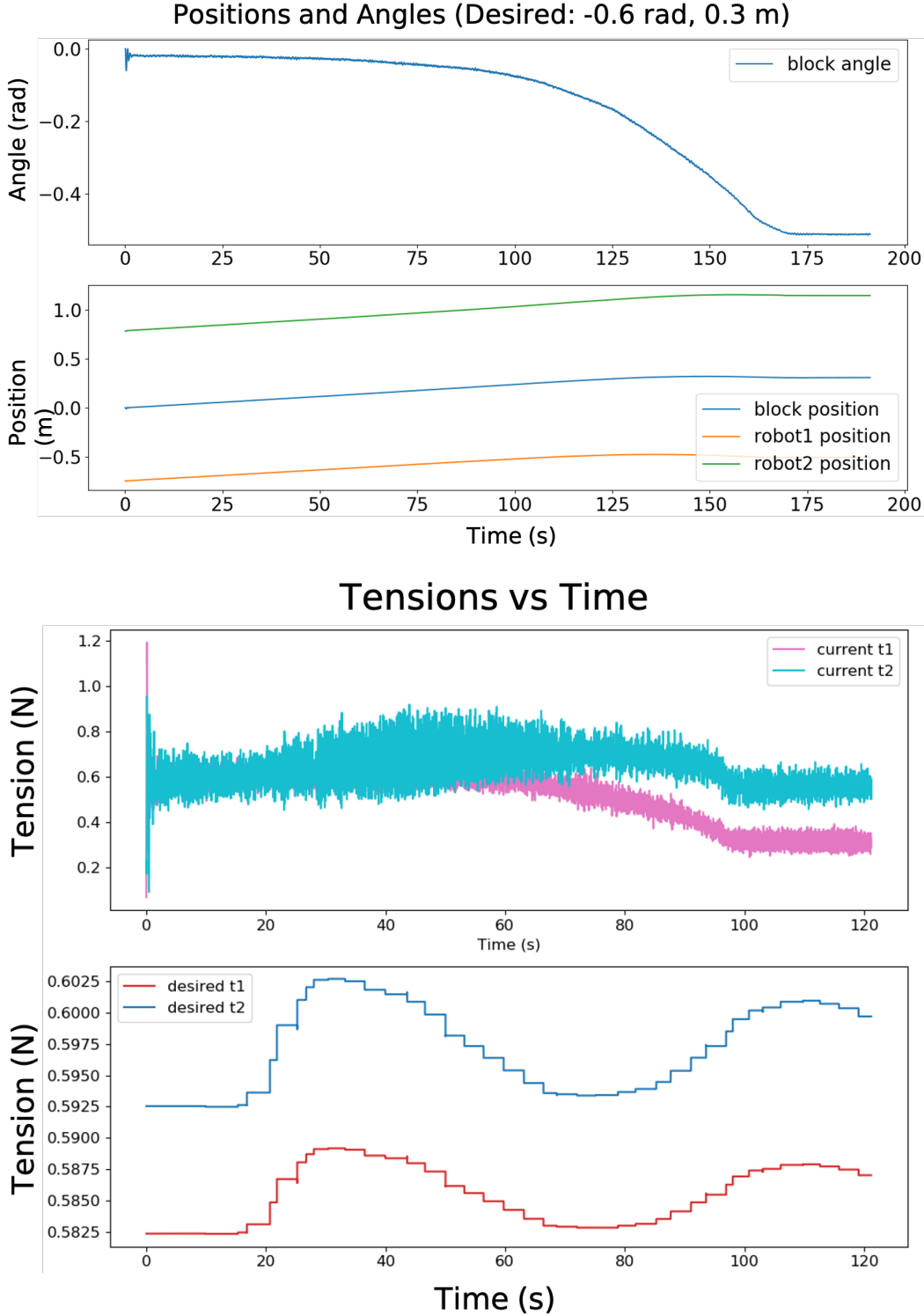


Figure 5.5: Plots of the results of telling the system to move the block object to position 0.3 along the x -axis and rotate it by -0.6 radians using the velocity controller.

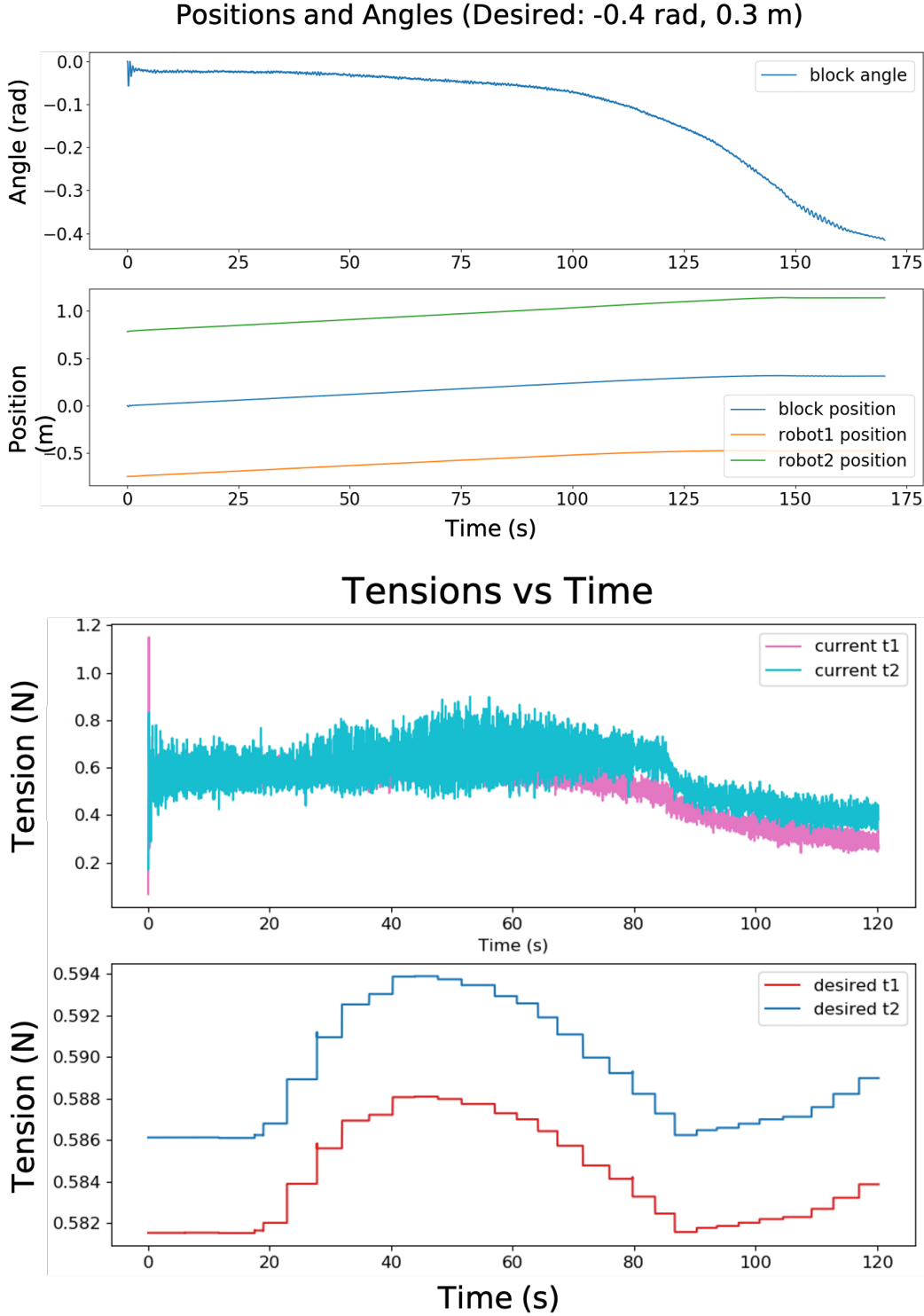


Figure 5.6: Plots of the results of telling the system to move the block object to position 0.3 along the x -axis and rotate it by -0.4 radians using the velocity controller.

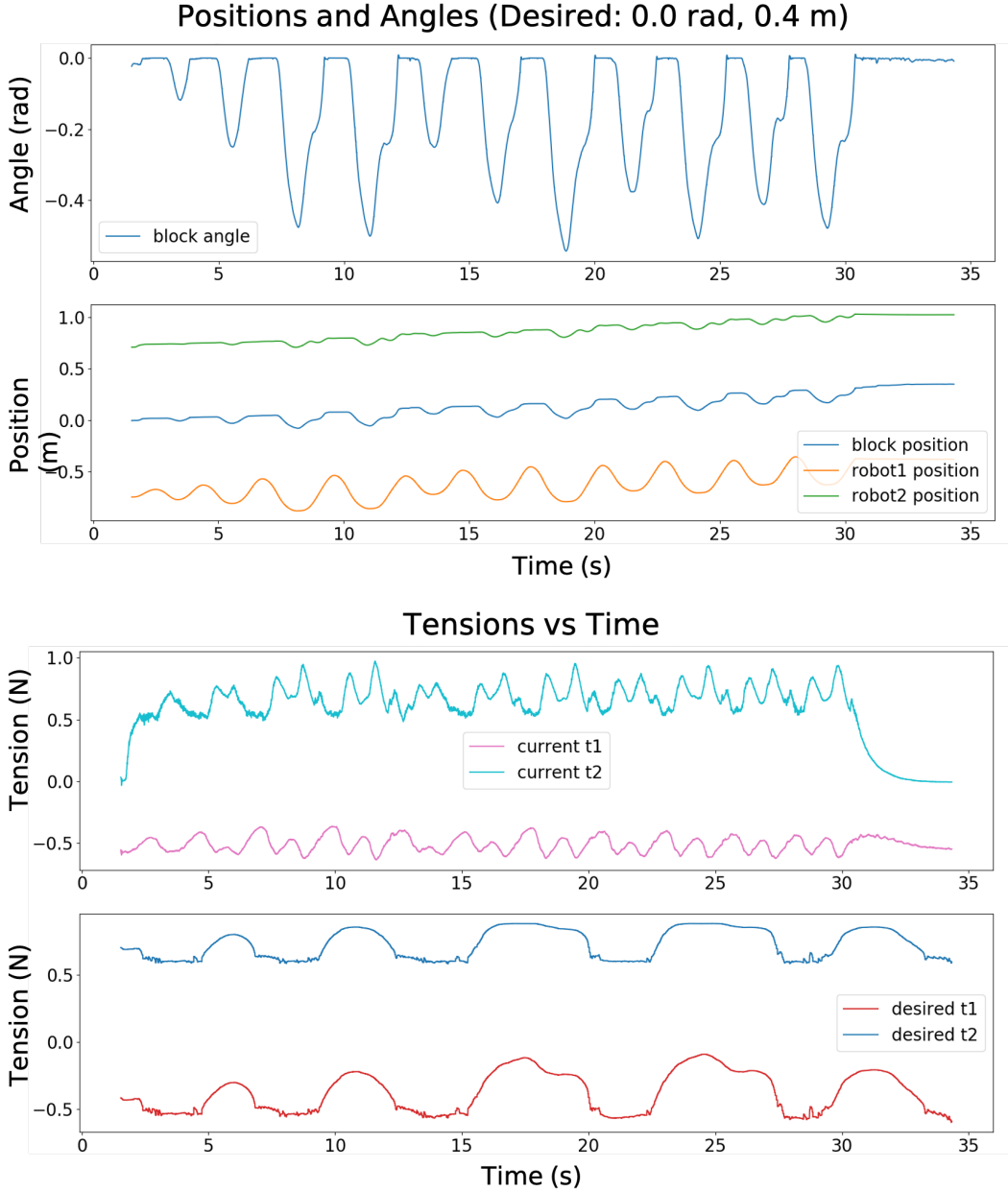


Figure 5.7: Plots of the results of pure translation of the object by 0.4 m using the torque controller. We can observe that the torque controller exhibits far more oscillatory behavior than the velocity controller. This is most likely due to a combination of a stick-slip friction phenomena, causing the robots to repeatedly need to overcome the force of friction between the block and the ground, as well as the torque controller over-correcting each time it misses its goal. The controller over-correcting could most likely be remedied with further tuning.

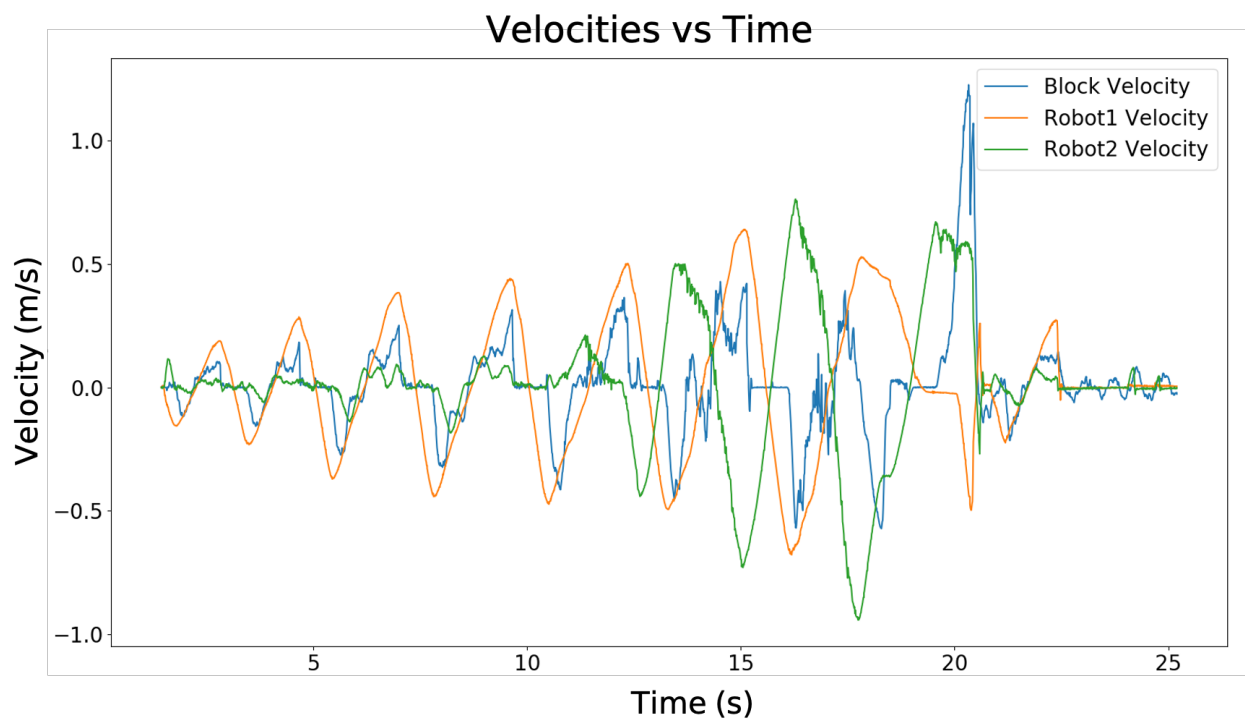


Figure 5.8: A plot of the velocity of the robots and block while translating the block 0.4 m using the torque controller.

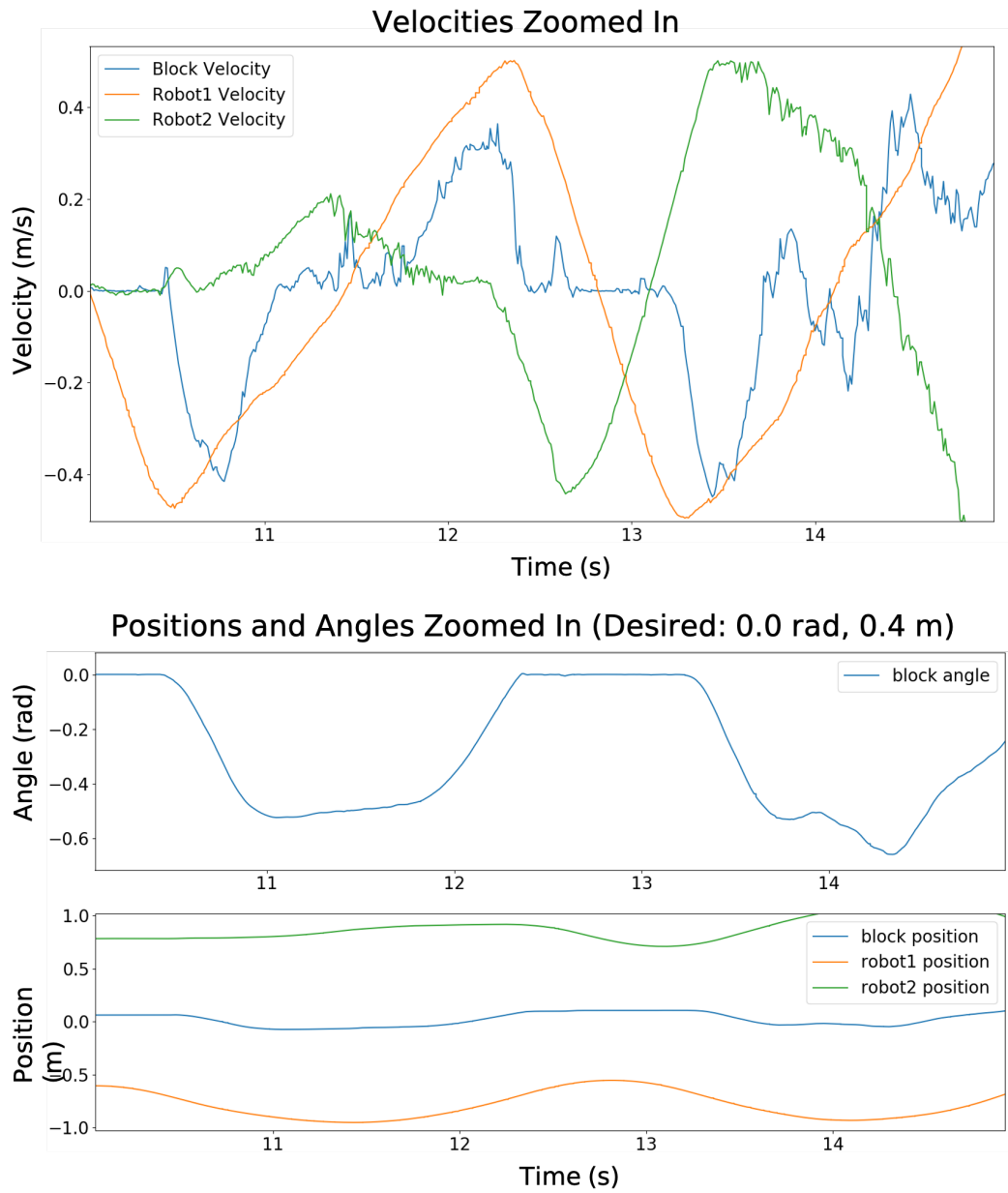


Figure 5.9: Close up snippets of the block angle, the block and robots' positions, and their velocities as the torque controller translates the block 0.4 m. Although only translation is requested, the angle of the block oscillates heavily as the block continuously tips back and forth due to the robots over-correcting in each direction.

Chapter 6

Discussion and Conclusion

Overall, the results of our experiments were favorable towards our overall goal of performing manipulation tasks on larger objects using millirobots rather than a large, bilateral arm mobile robot that would traditionally be used for such tasks. In most of the tests, the robots were able to successfully move the object and converge to the desired position and orientation.

While the velocity controller seemed to struggle slightly with reversing the direction of the robot when needing less tension on the object or when needing to translate it the opposite direction, the torque controller encountered similar problems much less frequently and had an easier time with such situations.

A limitation of our project, however, is that the object has a limited degree of freedom due to only having two robots and tethers attached to the block at fixed points. With more robots, the block could potentially be capable of a wider range of motions. Our model and experiments also only take two dimensions into account and do not account for three dimensional movement. Future work could work to remedy these shortcomings.

Another interesting addition for future work would also be to develop mechanisms for the robots to be able to attach the tethers to the object themselves at appropriate locations as well as being able to manipulate objects of various shapes and sizes. Since the masses of our object and each robot were 0.1 kg and 0.16 kg, respectively, the robots were able to produce enough force to successfully move the object. In order to move objects of greater mass, this set up can be scaled by using more robots to produce more forces or by having the robots attach the tethers to winches capable of producing enough tension on the tethers to perform the desired grasp and manipulation.

In conclusion, we have shown that the manipulation of objects that would normally be performed by large, expensive arm robots can also be executed by small, affordable millirobots working together or with winches and using tethers to exert the necessary forces on the object to grasp it. Our results have shown that our control scheme and environment set

up is able to successfully manipulate the object and converge to the target transformation. Further research into this subject could help produce small, affordable robots capable of manipulating objects and furniture much larger than them allowing them to assist people in their homes with household chores and organizational tasks. Such technology could greatly help many people, particularly adults who could then retain their independence when they might otherwise need constant in-home care.

Bibliography

- [1] Maya Cakmak and Leila Takayama. “Towards a comprehensive chore list for domestic robots”. In: *2013 8th ACM/IEEE International Conference on Human-Robot Interaction (HRI)*. 2013, pp. 93–94. DOI: [10.1109/HRI.2013.6483517](https://doi.org/10.1109/HRI.2013.6483517).
- [2] David L. Christensen et al. “Let’s All Pull Together: Principles for Sharing Large Loads in Microrobot Teams”. In: *IEEE Robotics and Automation Letters* 1.2 (2016), pp. 1089–1096. DOI: [10.1109/LRA.2016.2530314](https://doi.org/10.1109/LRA.2016.2530314).
- [3] Matthew A. Estrada et al. “Forceful Manipulation with Micro Air Vehicles”. In: *Science Robotics* 3.23 (2018). DOI: [10.1126/scirobotics.aau6903](https://doi.org/10.1126/scirobotics.aau6903). eprint: <https://robotics.sciencemag.org/content/3/23/eaau6903.full.pdf>. URL: <https://robotics.sciencemag.org/content/3/23/eaau6903>.
- [4] C. Ferrari and J. Canny. “Planning optimal grasps”. In: *Proceedings 1992 IEEE International Conference on Robotics and Automation*. 1992, 2290–2295 vol.3. DOI: [10.1109/ROBOT.1992.219918](https://doi.org/10.1109/ROBOT.1992.219918).
- [5] Jiaxin L. Fu and Nancy S. Pollard. “On the Importance of Asymmetries in Grasp Quality Metrics for Tendon Driven Hands”. In: *2006 IEEE/RSJ International Conference on Intelligent Robots and Systems*. 2006, pp. 1068–1075. DOI: [10.1109/IROS.2006.281812](https://doi.org/10.1109/IROS.2006.281812).
- [6] Joshua M. Inouye, Jason J. Kutch, and Francisco J. Valero-Cuevas. “A Novel Synthesis of Computational Approaches Enables Optimization of Grasp Quality of Tendon-Driven Hands”. In: *IEEE Transactions on Robotics* 28.4 (2012), pp. 958–966. DOI: [10.1109/TR0.2012.2196189](https://doi.org/10.1109/TR0.2012.2196189).
- [7] Joshua M. Inouye, Jason J. Kutch, and Francisco J. Valero-Cuevas. “A Novel Synthesis of Computational Approaches Enables Optimization of Grasp Quality of Tendon-Driven Hands”. In: *IEEE Transactions on Robotics* 28.4 (2012), pp. 958–966. DOI: [10.1109/TR0.2012.2196189](https://doi.org/10.1109/TR0.2012.2196189).
- [8] Cory D. Kidd and Cynthia Breazeal. “Robots at home: Understanding long-term human-robot interaction”. In: *2008 IEEE/RSJ International Conference on Intelligent Robots and Systems*. 2008, pp. 3230–3235. DOI: [10.1109/IROS.2008.4651113](https://doi.org/10.1109/IROS.2008.4651113).

- [9] I. Kim and H. Inooka. “Determination of Grasp Forces for Robot Hands Based on Human Capabilities”. In: *IFAC Proceedings Volumes* 26.2, Part 4 (1993). 12th Triennial World Congress of the International Federation of Automatic control. Volume 4 Applications II, Sydney, Australia, 18-23 July, pp. 979–984. ISSN: 1474-6670. DOI: [https://doi.org/10.1016/S1474-6670\(17\)48617-4](https://doi.org/10.1016/S1474-6670(17)48617-4). URL: <https://www.sciencedirect.com/science/article/pii/S1474667017486174>.
- [10] Richard M. Murray, Zexiang Li, and S. Shankar Sastry. *A Mathematical Introduction to Robotic Manipulation*. 1994.
- [11] Taylor Niehues et al. “Cartesian-Space Control and Dextrous Manipulation for Multi-Fingered Tendon-Driven Hand”. In: *2014 IEEE International Conference on Robotics and Automation (ICRA)*. 2014, pp. 6777–6783. DOI: [10.1109/ICRA.2014.6907860](https://doi.org/10.1109/ICRA.2014.6907860).
- [12] Ryuta Ozawa, Kazunori Hashirii, and Hiroaki Kobayashi. “Design and control of underactuated tendon-driven mechanisms”. In: *2009 IEEE International Conference on Robotics and Automation*. 2009, pp. 1522–1527. DOI: [10.1109/ROBOT.2009.5152222](https://doi.org/10.1109/ROBOT.2009.5152222).
- [13] Hossein Rastgoftar and Ella M. Atkins. “Cooperative aerial lift and manipulation (CALM)”. In: *Aerospace Science and Technology* 82-83 (2018), pp. 105–118. ISSN: 1270-9638. DOI: <https://doi.org/10.1016/j.ast.2018.09.005>. URL: <https://www.sciencedirect.com/science/article/pii/S127096381830912X>.
- [14] Hayley Robinson, Bruce MacDonald, and Elizabeth Broadbent. “The Role of Healthcare Robots for Older People at Home: A Review”. In: *International Journal of Social Robotics* 6.4 (2014). DOI: [10.1007/s12369-014-0242-2](https://doi.org/10.1007/s12369-014-0242-2). URL: <https://doi.org/10.1007/s12369-014-0242-2>.
- [15] D. Rus, B. Donald, and J. Jennings. “Moving furniture with teams of autonomous robots”. In: *Proceedings 1995 IEEE/RSJ International Conference on Intelligent Robots and Systems. Human Robot Interaction and Cooperative Robots*. Vol. 1. 1995, 235–242 vol.1. DOI: [10.1109/IR0S.1995.525802](https://doi.org/10.1109/IR0S.1995.525802).
- [16] Koushil Sreenath and Vijay Kumar. “Dynamics, Control and Planning for Cooperative Manipulation of Payloads Suspended by Cables from Multiple Quadrotor Robots”. In: June 2013. DOI: [10.15607/RSS.2013.IX.011](https://doi.org/10.15607/RSS.2013.IX.011).
- [17] Sean Wilson et al. “Multi-robot Replication of Ant Collective Towing Behaviours”. In: *Royal Society Open Science* 5.10 (2018). DOI: [10.1098/rsos.180409](https://doi.org/10.1098/rsos.180409). eprint: <https://www.ncbi.nlm.nih.gov/pmc/articles/PMC6227946/>. URL: <https://www.ncbi.nlm.nih.gov/pmc/articles/PMC6227946/>.
- [18] Jun Zeng et al. “Differential Flatness Based Path Planning With Direct Collocation on Hybrid Modes for a Quadrotor With a Cable-Suspended Payload”. In: *IEEE Robotics and Automation Letters* 5.2 (2020), pp. 3074–3081. DOI: [10.1109/LRA.2020.2972845](https://doi.org/10.1109/LRA.2020.2972845).